Origins of Activity Enhancement in Enzyme Cascades on Scaffolds

Ofer Idan and Henry Hess*

Department of Biomedical Engineering, Columbia University, New York, New York 10027, United States

ABSTRACT The concept of "metabolic channeling" as a result of rapid transfer of freely diffusing intermediate substrates between two enzymes on nanoscale scaffolds is examined using simulations and mathematical models. The increase in direct substrate transfer due to the proximity of the two enzymes provides an initial but temporary boost to the throughput of the cascade and loses importance as product molecules of enzyme 1 (substrate molecules of enzyme 2) accumulate in the surrounding container. The characteristic time scale at which this boost is significant is given by the ratio of container volume to the product of substrate diffusion constant and interenzyme distance and is on the order of milliseconds to seconds in some experimental systems. However, the attachment of a large number of enzyme pairs to a scaffold provides an increased number of local "targets", extending the characteristic time. If substrate molecules for enzyme 2 are sequestered by an alternative reaction in the container, a scaffold can result in a permanent boost to cascade throughput with a magnitude given by the ratio of the above-defined time scale to the lifetime of the substrate molecule in the container. Finally, a weak attractive interaction between substrate molecules and the scaffold creates a "virtual compartment" and substantially accelerates initial throughput. If intermediate substrates can diffuse freely, placing individual enzyme pairs on scaffolds is only beneficial in large cells, unconfined extracellular spaces or in systems with sequestering reactions.

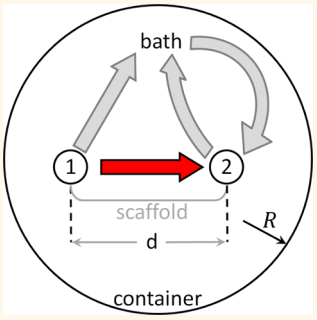

KEYWORDS: enzyme cascades · nanobiotechnology · DNA scaffolds · transport processes · mathematical modeling

Enzyme scaffolds enable the precise placement of components of enzymatic cascades within nanometer distances.[1−3] Recent experimental results demonstrate significantly increased throughput of enzymatic cascades as a result of the utilization of a scaffold, but the basis for this increase is not understood.[4−9] Here, the concept of "metabolic channeling" as a result of nanometer separations between enzymes on scaffolds is examined using simulations and mathematical models.

Scaffolds are involved in many signaling pathways and metabolic processes and can be potentially advantageous for a number of reasons.[2,10] A frequently cited reason is "substrate channeling": the direct transfer of intermediates between enzymes in the cascade without the release of the intermediate into the bulk solution.[11] While substrate channeling can occur as a result of distinct structural features of the enzymes, such as tunnels or electrostatic "highways" for substrates,[12] it has been suggested,[13] but later challenged with experiments,[14−17] that merely linking enzymes can increase the throughput of an enzyme cascade due to facilitated transport. In recent years there has been a growing interest in scaffolds and enzymatic cascades for synthetic biology and biofuel production.[10,18]

The construction of artificial enzyme scaffolds with precise dimensions on the nanometer scale has been facilitated by recent advances in DNA, RNA, and protein nanotechnology. Wilner *et al.* used a DNA scaffold to tether sequential enzymes and systematically vary the interenzyme distance (Figure 1A). When the two enzymes were separated by 6 nm, a 16-fold increase in product formation rate was observed compared to untethered enzymes.[5] Delebecque *et al.* created artificial RNA scaffolds in bacteria which recruited specific enzymes from the cytosol and increased the output of the cascade formed by the recruited enzymes 48-fold (Figure 1B).[6] Fu *et al.* bound enzymes and a "bridge" protein to DNA tiles, creating a hydration layer around the enzymes, thereby increasing the reaction rate (Figure 1C).[8] A protein scaffold was used by Dueber *et al.*, who used protein−protein interaction domains to bind three enzymes in a cascade (Figure 1D).[4] The number of repeats for each enzyme was altered to achieve the optimal reaction rate by increasing the number of rate-limiting enzymes.

* Address correspondence to hh2374@columbia.edu.

Received for review June 4, 2013 and accepted September 5, 2013.

Published online September 05, 2013
10.1021/nn402823k

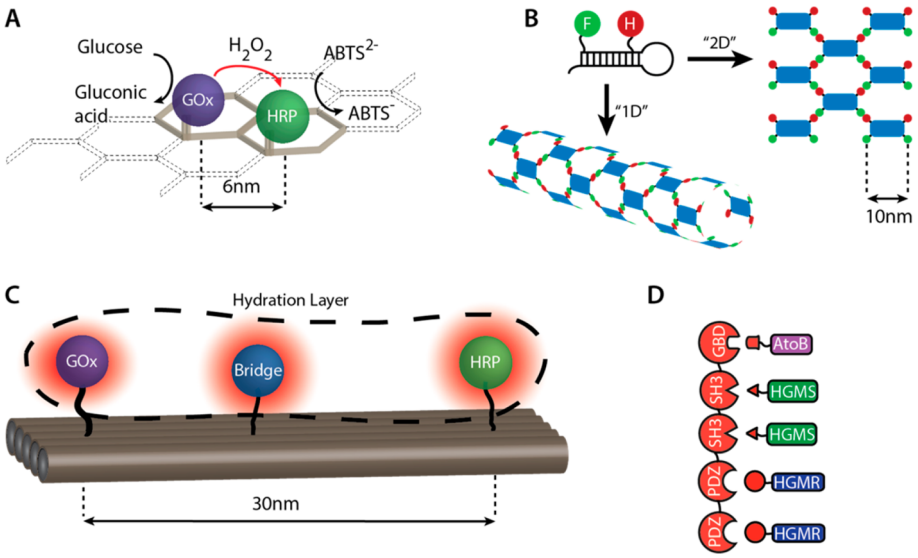

Figure 1. Schematics of enzyme cascades on scaffolds described in the literature. (A) Glucose oxidase (GOx), horseradish peroxidase (HRP) pairs attached to a DNA "ribbon" with hexagonal cells;[5] (B) Ferrodoxin (F), hydrogenase (H) pairs tethered to RNA tiles which are assembled into different patterns;[6] (C) GOx-HRP pairs attached to DNA tiles with a noncatalytic protein inserted between the enzymes to induce intermediate substrate propagation;[8] (D) Artificial scaffold comprised of protein–protein interaction domains recruits endogenous and foreign enzymes in a bacterium.[4] (Reprinted from Idan, O.; Hess, H. Engineering enzymatic cascades on nanoscale scaffolds. *Current Opinion in Biotechnology* 2013, *24* (4), 606–611; Copyright (2013) with permission from Elsevier.)

Our goal is to (1) calculate if the precise nanoscale arrangement of enzymes can yield benefits even if the molecules diffuse freely from one enzyme to the next in the reaction cascade and (2) contrast this with the situation where the substrate molecules are attracted to the scaffold.

RESULTS AND DISCUSSION

In the absence of a scaffold, the throughput of an enzyme cascade, where each enzyme follows Michaelis–Menten kinetics, can be easily calculated. The steady-state throughput is determined by the slowest enzyme in the cascade, and initially the product concentration increases with the *n*th power of time for a reaction cascade comprising *n* enzymes working in sequence. In particular, a cascade of two enzymes should show initially a quadratic increase of product concentration with time in the absence of other reactions (Figure 2).

In scaffold systems, the steady state throughput is still determined by the maximum reaction rate of the slowest enzyme in the cascade. However, the initial throughput can be increased by the scaffold. This increase has been suggested to arise from the increased probability that a product molecule released by enzyme 1 will find its way directly to enzyme 2 positioned in the immediate vicinity.[5,8] For diffusive transport to a spherical adsorber with radius r from a starting point at a distance d from the center of the adsorber the probability to reach the adsorber is given by the ratio r/d,[19] suggesting that a scaffold that places enzyme 1 within a few nanometers of enzyme 2 might have a major benefit for the throughput. To obtain a more detailed picture, we have simulated random walks of a substrate molecule starting at a defined distance from a spherical target (representing the target enzyme) located in the center of a spherical container. The random walks are terminated when the molecule encounters the surface of the spherical target (a "direct" trajectory) or the surface of the container. The fraction f_{direct} of direct trajectories to the target increases, as expected, roughly in proportion to the inverse distance, for example, from f_{direct} = 2.3% at an initial distance of 100 nm to f_{direct} = 27% at an initial distance of 10 nm (Figure 3A,B).

The direct trajectories will substantially contribute to the throughput of the cascade if the direct flux dominates over the flux resulting from substrate molecules which are lost to the container and subsequently return. If the initial concentration of the substrate of enzyme 2 in the container is zero, the direct flux dominates for a certain time. As the substrate concentration increases in the container, there will be a time point after which the direct trajectories make a smaller contribution to the formation of product than the population of substrate molecules in the container.

This time point can be estimated by dividing the flux of substrates emitted from enzyme 1 into a direct stream to enzyme 2 and a stream of molecules into the container (Figure 3C). At substrate concentrations far below the K_m of enzyme 2, the two streams do not interfere and the rate k_2 of product formation is approximately

$$k_2 = Ef_{direct}k_1 + k_{cat,2}\frac{[S_2]}{K_{m,2}} \quad (1)$$

Here $E = k_{cat,2}/K_{m,2}k_{dif}$ is the efficiency of enzyme 2 at vanishing substrate concentration;[20] k_1 is the rate at which enzyme 1 is releasing its product (serving as

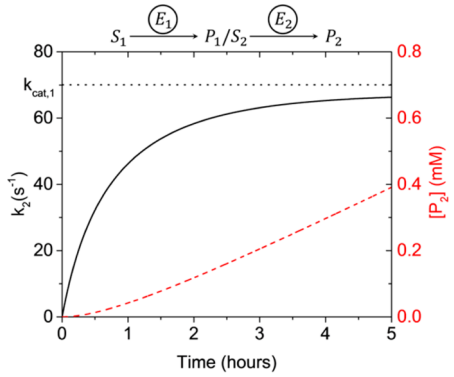

Figure 2. Reaction rate and final product concentration of a cascade of two enzymes in the absence of a scaffold. Initially, the reaction rate (black solid line) increases linearly and the product concentration (red dashed line) quadratically with time. On a time scale of hours, the system reaches a steady state and the reaction rate reaches the maximum reaction rate (here limited by the constant production rate of enzyme 1). In this example, the enzyme concentrations are 0.4 nM for both enzymes, and the kinetic parameters of enzymes 1 and 2 are equal to those of GOx and HRP, respectively (stated in Methods). At this concentration, the average distance between a GOx and a HRP molecule is approximately 1 μm.

substrate for enzyme 2); $k_{cat,1,2}$ are the turnover numbers and $K_{m,2}$ is the Michaelis constant of enzyme 2; $[S_2]$ is the average concentration of the substrate of enzyme 2 in the container; k_{dif} is the diffusion-limited reaction rate. It is assumed that $[S_2] \ll K_{m,2}$, because we focus on the initial reaction rate in the container.

The second term begins to exceed the first term when

$$[S_2] = \frac{Ef_{direct}k_1K_{m,2}}{k_{cat,2}} \quad (2)$$

Estimating the average concentration of the substrate of enzyme 2 in the container as $[S_2] \approx (1 - Ef_{direct})k_1t/VN_A$, where $1 - Ef_{direct}$ is the fraction of substrate molecules produced by enzyme 1 which is not directly processed by enzyme 2, V is the volume of the container, and t is the time elapsed, we obtain

$$t = \frac{Ef_{direct}K_{m,2}VN_A}{(1 - Ef_{direct})k_{cat,2}} \quad (3)$$

Estimating $f_{direct} \approx r_2/d$, where r_2 is the radius of enzyme 2 and d is the distance between the centers of enzymes 1 and 2,[19] using the definition for E and assuming $E \ll 1$ we obtain

$$t = \frac{r_2VN_A}{(d - Er_2)k_{dif}} \approx \frac{r_2VN_A}{dk_{dif}} \quad (4)$$

Using $k_{dif} \approx 4\pi r_2D_{substrate}N_A$, because substrate molecules are small and diffuse fast relative to the enzyme,[21] we obtain

$$t \approx \frac{V}{4\pi D_{substrate}d} \quad (5)$$

This is an interesting result because the characteristic time does not depend on the catalytic properties of the enzymes. A scaffold noticeably increases throughput over a time scale which is only dependent on the geometry of the system (volume of the container and size of the scaffold) and the diffusivity of the substrate traveling from one enzyme to the next. For a volume of 10^3 μm^3 corresponding to the volume of a mammalian cell, a diffusion coefficient of 10^{-3} $\mu m^2/s$ corresponding to a small molecule diffusing in water, and an enzyme separation of 10 nm, the time scale is on the order of 10 s. For smaller volumes such as those of mitochondria or bacteria ($V = 0.1-10$ μm^3), a scaffold provides almost no benefit over free-floating enzymes.

To check this simple model, we solved the reaction-diffusion equation for the substrate of enzyme 2, S_2:

$$\frac{d[S_2]}{dt} + \nabla \cdot (-D\nabla[S_2]) = 0 \quad (6)$$

The two enzymes are modeled as spheres that are placed at defined locations in a large spherical container. The vessel wall is modeled as a reflecting boundary, and an influx/outflux boundary condition is imposed on the respective enzyme walls. The influx is constant over time and equal to k_1; the outflux is dictated by local Michaelis–Menten kinetics:

$$k_2 = k_{cat,2}\frac{\overline{[S_2]}}{K_{m,2} + \overline{[S_2]}} \quad (7)$$

where bars indicate averages over the enzyme surface. The parameters used in the simulations were selected to match a previously described experiment, with hydrogen peroxide produced by glucose oxidase and consumed by horseradish peroxidase.[5] The simulations confirm our estimate and show that the direct path loses its dominance as the vessel fills up with substrate molecules (Figure 4A–C). The interenzyme distance, which is defined by the scaffold size, determines the magnitude of the reaction rate reached after the first microsecond (Figure 4D). This initial reaction rate increases with decreasing scaffold size because more substrate molecules take the direct route to enzyme 2 (Figure 3). An increase in the vessel volume (or the average volume per enzyme pair) delays the impact of the indirect path because more time is required to build up a substantial concentration of substrate molecules (Figure 4E). A decrease in the diffusion coefficient without a change in the turnover number and Michaelis constant of enzyme 2 increases the initial reaction rate (Figure 4F) because it decreases the collision rate, thereby implicitly increasing the efficiency of enzyme 2. Our simulations also show that placing the two enzymes a few nanometers apart makes a negligible contribution to product formation on a time scale of seconds.[22]

One of the explanations for the increase in throughput of scaffold systems observed in recent experiments is that engineered scaffolds often aggregate a large number of enzyme pairs due to their "ribbon" structure

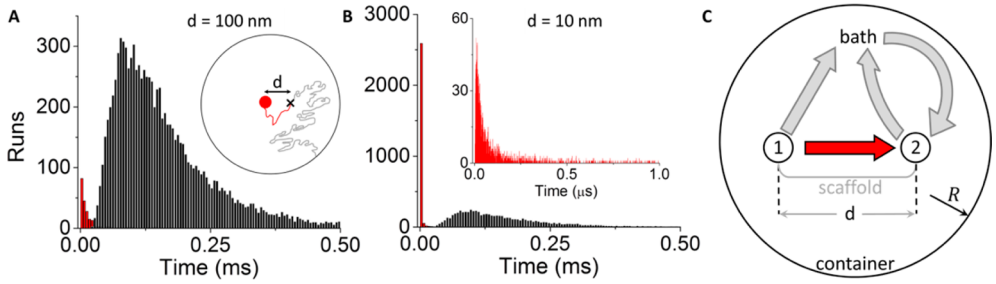

Figure 3. Monte Carlo simulations of diffusive transport. (A) Random walks from a point source (representing enzyme 1 in a cascade) toward a sphere (representing enzyme 2, $r = 2.8$ nm) from an initial distance $d = 100$ nm with diffusion coefficient $D = 10^{-5}$ cm^2/s. A fraction ($f = 2.3\%$) of the 10000 trajectories arrives first at the sphere (red) and the remainder arrives first at the boundary of the container with radius $R = 1000$ nm (black). (B) Decreasing the distance between the enzymes to $d = 10$ nm increases the fraction of trajectories arriving first at the sphere ($f = 27\%$). Inset: The arrival time distribution at short times. (C) The molecules released from enzyme 1 can be conceptually separated into a "direct" stream toward enzyme 2 (red) and a stream into the surrounding bath (gray). A small catalytic efficiency of enzyme 2 diverts most of the direct stream to the bath.

(Figure 1A,B).[5,6] A rough approximation of the effect of placing thousands of enzyme pairs in close proximity is to consider them as one enzyme pair with a proportional increase in the turnover numbers.[22] Then, eq 5 applies and predicts an enhanced throughput for a time which increases in proportion to the number of the enzyme pairs, because the volume per ribbon is proportionally larger than the volume per enzyme pair.

To approximate such experimental systems more closely, we constructed a simulation with a ribbon-like structure in the shape of a torus (Figure 5). The minor radii of the toroids are the radii of the respective enzymes and the major radius of both is based on the scaffold's radius of gyration, $R_g = ((N_{seg})^{1/2}b)/\sqrt{6}$, where N_{seg} is the number of segments in the scaffold based on a $b = 100$ nm Kuhn length of a hexagonal DNA scaffold modeled as a freely jointed chain.

The benefit of the scaffold, which is negligible for individual enzymes, remains significant for a ribbon even on a time scale of seconds to minutes (Figure 5). However, this is primarily due to the large increase of the number of target enzymes in the general vicinity of each enzyme 1 molecule, and not because of the precise placement of enzyme 2 relative to enzyme 1. In addition, the dependence of the increase on the separation distance is smaller compared to our previous model. This matches the experimental results of Wilner *et al.* more closely, where the presence of a scaffold makes a significant contribution over a non-scaffold system, but the dimensions of the scaffold have a relatively small effect.[5] This effect could solely account for the observed increase, with a certain enzyme packing, or contribute in combination with other effects discussed in the next sections.

Another explanation for the enhanced throughput of an enzyme cascade on a scaffold is the loss of intermediates due to auto-oxidation or another sequestering reaction. Many intermediate compounds can be highly reactive in solution, especially in a cellular environment where many species are likely to react with, and thus sequester, the intermediate substrate intended for enzyme 2. In nanosystems using enzymes, sequestration of control molecules has been exploited to localize activation.[23] These systems arrive at a steady state much faster than systems without a sequestering reaction, in the case of the GOx-HRP system on the order of a few seconds. The benefit of the scaffold can be expressed as the ratio of the production rates of a scaffold and free systems: (full derivation is presented in the SI):

$$\frac{k_{2,\,scaf}}{k_{2,\,free}} = 1 + \frac{V}{4\pi Dd}R \qquad (10)$$

Results of a simulation incorporating a sequestration reaction are shown in Figure 6. As can be seen from the inset a sharp concentration gradient is generated in the vicinity of the source enzyme which does not dissipate for a long time. The ratio $k_{2,scaf}/k_{2,free}$ decreases rapidly toward its steady-state value of 1.034, 1.34, and 4.4 for $R = 1$ s^{-1}, $R = 10$ s^{-1}, and $R = 100$ s^{-1}, respectively, as predicted by eq 10. In summary, a scaffold can result in a permanent boost to scaffold throughput if substrate molecules for enzyme 2 are sequestered by an alternative reaction in the container, and the magnitude of the acceleration is given by the ratio of the time scale defined by eq 5 to the lifetime of the substrate molecule in the container ($1/R$).

Finally, the affinity of hydrogen peroxide for protein surfaces has been previously suggested to be responsible for the scaffold-related enhancement in throughput,[24,25] and a recent scaffold experiment where a protein placed in between enzyme 1 and 2 leads to an increase in throughput seems to confirm the concept.[8] This phenomenon suggests that attractive interactions between substrate molecules and enzymes/scaffolds are a potential driver for the increase in throughput observed in these systems. Again we aim to show that the behavior of the system can be captured by a simple model. To describe this process, we conceptually envelop a pair of enzymes with a semipermeable spherical barrier for the intermediate substrate. The probability of a substrate molecule to cross the barrier is reduced in proportion

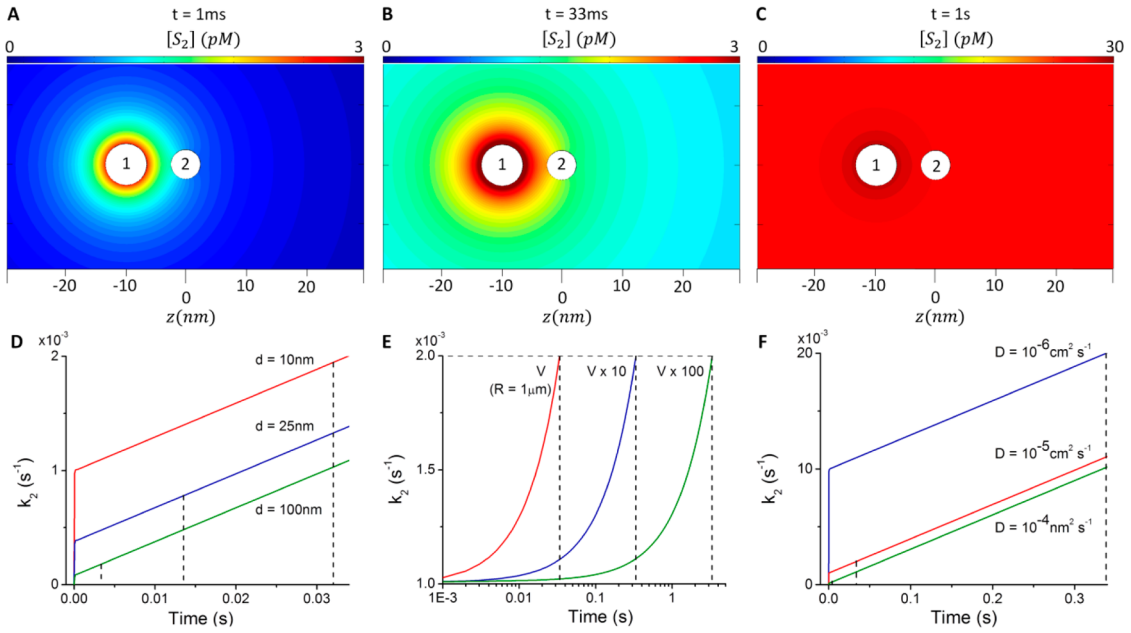

Figure 4. Results of a reaction-diffusion simulation of a GOx − HRP cascade. (A−C) Surface plots of the intermediate substrate concentration in the vicinity of the enzymes. (A) At short times the direct path provides the majority of substrate particles arriving at enzyme 2. (B) At the characteristic time the flux from the concentration of substrate in the vessel equals that from the direct path. (C) At longer times, the concentration of substrate in the vessel is high and nearly independent of location, and the direct path makes a negligible contribution. (D−F) Variation of the parameters affecting the characteristic time directly affects the production rate of enzyme 2. As shown in eq 5, the interenzyme distance (D) and diffusion coefficient (F) are inversely proportional to the characteristic time while the vessel volume (E) is proportional to it. Dotted lines indicate the time points where direct and indirect fluxes are equal. Unless noted otherwise the parameters used were $d = 10$ nm, $D = 10^{-5}$ cm^2/s, $R = 1000$ nm. Enzyme parameters are described in Methods.

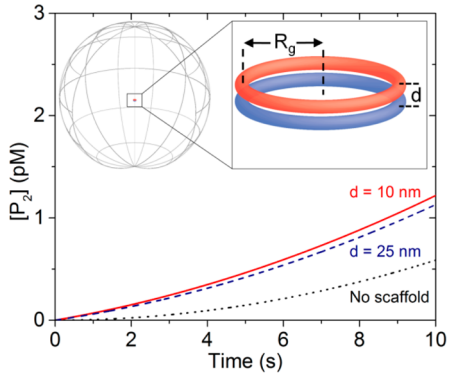

Figure 5. Reaction-diffusion simulations for 10000 GOx−HRP pairs on a folded scaffold. A simulation of a folded scaffold as two rings with a radius equal to the radius of gyration of a DNA hexagonal ribbon, $R_g = 1.3$ μm. Similar to the experimental results of Wilner *et al.*,[5] the presence of the scaffold significantly increases the rate of product formation, but the increase is only weakly dependent on the interenzyme distance. The container volume is the solution volume per pair multiplied by the number of enzymes on the scaffold, yielding a container radius of 21.5 μm. System parameters are described in Methods.

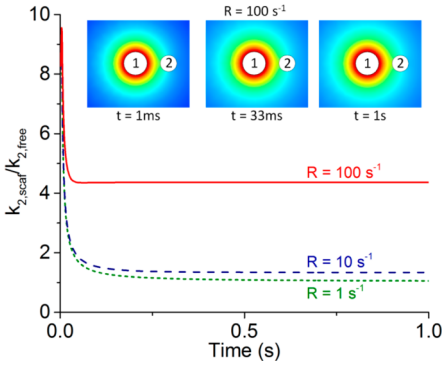

Figure 6. Reaction-diffusion simulations for enzyme pairs with a sequestering reaction. A higher sequestering reaction rate decreases the lifetime of the intermediate substrate. The concentration of the intermediate substrate is only significant in a small volume around the first enzyme. The ratio of reaction rates, $k_{2,scaf}/k_{2,free}$, increases with increased sequestration rate as predicted by eq 10. The container radius is 1.2 μm, corresponding to 0.2 nM as used in (5). Enzyme parameters are described in Methods.

to the Arrhenius factor $\exp(E_b/kT)$ and leads to an increase in the local concentration of substrate molecules, which in turn enhances the production rate of enzyme 2. The intermediate substrate concentration in the smaller compartment increases rapidly and the throughput reaches half its maximum ($k_2 = k_1/2$) after a time $t_{1/2}$ given by (see SI for full derivation)

$$t_{1/2} = \frac{K_{m,2}}{2k_{cat,2} - k_1} V'' e^{-E_b/kT} \qquad (13)$$

where E_b is the binding energy between scaffold/enzymes and the intermediate substrate and V'' is the volume of the container. The size of the "virtual"

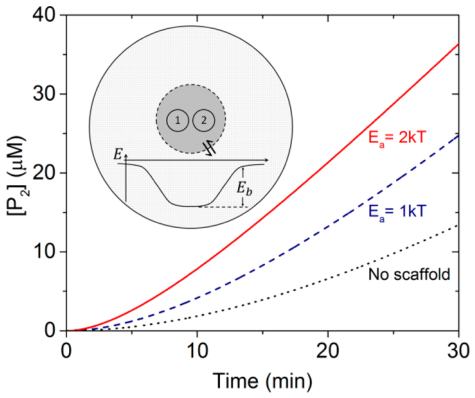

Figure 7. Simulations of the compartment model for different barrier energies. For a spherical compartment with a 20 nm radius, an energy barrier on the order of a few kT increases production rate compared to a nonscaffold system. This increase is evident on time scales of minutes and hours. The time to reach half the maximum speed can be approximated by eq 13 and is ~4 min for a barrier of 2 kT, 12 min for a barrier of 1 kT, and 30 min for a no-scaffold system (see Figure 1). The enzyme concentrations are 0.2 nM for both enzymes, and the kinetic parameters of enzyme 1 and 2 are equal to those of GOx and HRP, respectively (stated in Methods).

compartment created by the attractive interaction between substrate molecules and scaffold/enzymes does not affect the persistence of the enhancement effect (see SI).

A numerical solution of the reaction equations confirms the intuition that the local substrate concentration increases relative to the substrate concentration in the container roughly in proportion to the Arrhenius factor and gives a sustained boost to the cascade throughput irrespective of the size of the compartment.

Due to the exponential dependence of the Arrhenius factor on the binding energy, already a modest attractive interaction with binding energy of 1 or 2 kT substantially increases the local substrate concentration in the vicinity of the enzymes and the throughput of the cascade (Figure 7). For comparison, several small molecule substrates of HRP have binding energies to DNA between 3 and 20 kT.[16] This increase persists on a time scale of hours and not just seconds as the increase in throughput calculated for freely diffusing substrate molecules eq 5.

CONCLUSIONS

The throughput of sequential enzymatic reactions can be enhanced by spatial organization, for example, by localization into microcompartments.[26−28] While the concept of increasing throughput by placing enzymes close together is intuitively appealing,[29,30] we show that, for freely diffusing reactants, cascade throughput is only enhanced in very large containers, such as mammalian cells[31] or the extracellular environment of the cellulosome,[32,33] and only for a limited time. Of course, cellular scaffolds often support enzymatic cascades in which reactants are not permitted to diffuse freely,[10,34] but recent engineered scaffolds aim to support reaction sequences with freely diffusing substrates.[4−6] Rather than the proximity between two sequential enzymes, the aggregation of large numbers of enzymes on a scaffold enhances throughput by providing multiple targets for the diffusing substrate. If substrate molecules for enzyme 2 are sequestered by an alternative reaction in the container, a scaffold can result in a permanent boost to cascade throughput with a magnitude given by the ratio of the time scale defined by eq 5 to the lifetime of the substrate molecule in the container. Finally, a weak attractive interaction between substrate molecules and the scaffold creates a "virtual compartment" and substantially accelerates initial throughput.

METHODS

Random Walk Simulations. Random walk simulations were performed using MATLAB software (MathWorks Inc.). At the beginning of each iteration a particle was initialized at a specific distance d away from the center of an inner sphere with radius of 2.8 nm, which is the sum of the radii of the enzyme and the substrate molecule. The particle then performs a random walk on a 3-dimensional square grid with 0.1 nm step size. The iteration is terminated when the particle reaches either the inner sphere or crosses an outer sphere of radius 1000 nm and the number of step sizes is recorded. A total of 10000 iterations were conducted for each starting distance. Histograms of the arrival time to the inner and outer spheres were generated calculating the time steps according to $\Delta t = \Delta x^2/6D$, where Δx = 0.1 nm is the step size and $D = 10^9$ nm^2/s is the diffusion coefficient of hydrogen peroxide in water at 25 °C.[35]

Reaction-Diffusion Simulations. Using COMSOL Multiphysics finite element analysis software (COMSOL), a simulation of the enzyme cascade was constructed using the "transport of diluted species" module.

Enzyme Pair Simulations. A sphere representing enzyme 1 was placed in the center of a spherical container, and a sphere representing enzyme 2 was placed a distance d from the center. The enzyme parameters were based on the experimental system described by Wilner *et al.*[5] using glucose oxidase (GOx) from *Aspergillus niger* (r_1 = 3.5 nm,[36] $k_{cat,1}$ = 70 s^{-1}, obtained from averaging several values from www.brenda-enzymes.org to match values observed in ref 5, $K_{m,1}$ = 4 mM[37]) as enzyme 1 and horseradish peroxidase (HRP) from *Armoracia rusticana* (r_2 = 2.5 nm,[38] $k_{cat,2}$ = 200 s^{-1},[39] $K_{m,2}$ = 0.18 mM[40]) for enzyme 2. The diffusion coefficient of D = 10^9 nm^2/s used is the coefficient for hydrogen peroxide in water at 25 °C.[35] The outer boundary is set as a reflective boundary and the fluxes through the surfaces of the spheres were set as equal to $\phi_1 = k_1/4\pi r_1^2 N_A$ for enzyme 1 (influx to the container) and equal to $\phi_2 = k_{cat,2}\,([S_2]/(K_{m,2} + [S_2])) \cdot 1/(4\pi r_2^2 N_A)$ for enzyme 2 (outflux from the container) where $[S_2]$ is the average concentration of the intermediate substrate on the surface of the sphere representing enzyme 2. The product concentration was determined by numerically integrating k_2 over time. The system was solved as a 2D axisymmetric model, where the solution domain is a half circle with a symmetry axis. After obtaining a 2D solution, the software extrapolated a 3D solution by rotation of the system around the symmetry axis. A free tetrahedral mesh with a 0.01 nm size constraint on the enzyme surfaces was used.

Torus Simulations. Two toroids were constructed with minor radii dictated by the enzyme radii stated above, and the

major radius of both toroids was calculated using $R_g = (N_{seg})^{1/2}b/\sqrt{6}$. N_{seg} was calculated using $N_{seg} = N_e \cdot d_{vert}/b$, where N_e = 10000 is the number of enzymes on the scaffold, d_{vert} = 10 nm is the center-to-center separation between enzyme pairs on the scaffold, and b = 100 nm is the Kuhn length calculated for a dsDNA modeled as a freely jointed chain. The fluxes of the toroids have been changed to reflect the new geometry: $\phi_1 = N_e \cdot k_1 \cdot (1/(4\pi^2 r_1 R_g N_A))$ and $\phi_1 = N_e k_{cat,2}$ $([S_2]/(K_{m,2} + [S_2]) \cdot (1/(4\pi^2 r_2 R_g N_A)))$, where $[S_2]$ is now calculated over the surface of torus 2.

Sequestering Reactions. To describe the conversion of substrate 2 by a side reaction with a spatially and temporally constant rate R, the enzyme pair simulations were modified by adding a term $-R[S_2]$ to the differential equation describing the time-evolution of the concentration of substrate 2, $[S_2]$.

Solutions of ODE Systems. The ordinary differential equations describing the system are usually not analytically tractable. Using the ODE solvers in MATLAB, ode45 and ode15 we solved for the intermediate substrate concentration, reaction rate and final product concentration for the different setups.

Free Enzyme Pairs. System and enzyme parameters used were the same as in the reaction-diffusion simulations. The equations of the free system are

$$N_A V \frac{d[S_2]}{dt} = \overbrace{k_{cat,1} \frac{[S_1]}{K_{m,1} + [S_1]}}^{\approx k_{cat,1} = k_1} - k_{cat,2} \frac{[S_2]}{K_{m,2} + [S_2]}$$

$$k_2 = k_{cat,2} \frac{[S_2]}{K_{m,2} + [S_2]}$$

Sequestering Reactions. For a system with a sequestering side reaction, we added the reaction term $-R[S_2]$ to the equation for the intermediate substrate.

Compartmentalization Model. See SI for full description of the system and the equations associated with it.

Conflict of Interest: The authors declare no competing financial interest.

Supporting Information Available: Detailed equations, derivations, and calculations for free-floating, scaffold, sequestration, and compartmentalization models. This material is available free of charge *via* the Internet at http://pubs.acs.org

Acknowledgment. Helpful discussion with Jose Blanchet and Jonathan Dworkin and financial support from NSF Grant DMR 1015486 are gratefully acknowledged.

REFERENCES AND NOTES

1. Lim, W. A. Designing Customized Cell Signalling Circuits. *Nat. Rev. Mol. Cell Biol.* **2010**, *11*, 393–403.
2. Zhang, Y. H. P. Substrate Channeling and Enzyme Complexes for Biotechnological Applications. *Biotechnol. Adv.* **2011**, *29*, 715–725.
3. Idan, O.; Hess, H. Engineering Enzymatic Cascades on Nanoscale Scaffolds. *Curr. Opin. Biotechnol.* **2013**, *24*, 606–611.
4. Dueber, J. E.; Wu, G. C.; Malmirchegini, G. R.; Moon, T. S.; Petzold, C. J.; Ullal, A. V.; Prather, K. L. J.; Keasling, J. D. Synthetic Protein Scaffolds Provide Modular Control Over Metabolic Flux. *Nat. Biotechnol.* **2009**, *27*, 753–759.
5. Wilner, O. I.; Weizmann, Y.; Gill, R.; Lioubashevski, O.; Freeman, R.; Willner, I. Enzyme Cascades Activated on Topologically Programmed DNA Scaffolds. *Nat. Nanotechnol.* **2009**, *4*, 249–254.
6. Delebecque, C. J.; Lindner, A. B.; Silver, P. A.; Aldaye, F. A. Organization of Intracellular Reactions with Rationally Designed RNA Assemblies. *Science* **2011**, *333*, 470–474.
7. Zhang, L.; Shi, J. F.; Jiang, Z. Y.; Jiang, Y. J.; Qiao, S. Z.; Li, J. A.; Wang, R.; Meng, R. J.; Zhu, Y. Y.; Zheng, Y. Bioinspired Preparation of Polydopamine Microcapsule for Multienzyme System Construction. *Green Chem.* **2011**, *13*, 300–306.
8. Fu, J.; Liu, M.; Liu, Y.; Woodbury, N. W.; Yan, H. Interenzyme Substrate Diffusion for an Enzyme Cascade Organized on Spatially Addressable DNA Nanostructures. *J. Am. Chem. Soc.* **2012**, *134*, 5516–5519.
9. Xin, L.; Zhou, C.; Yang, Z.; Liu, D. Regulation of an Enzyme Cascade Reaction by a DNA Machine. *Small* **2013**, 10.1002/smll.201300019.
10. Good, M. C.; Zalatan, J. G.; Lim, W. A. Scaffold Proteins: Hubs for Controlling the Flow of Cellular Information. *Science* **2011**, *332*, 680–686.
11. Schoffelen, S.; van Hest, J. C. M. Multi-Enzyme Systems: Bringing Enzymes Together *In Vitro*. *Soft Matter* **2012**, *8*, 1736–1746.
12. Miles, E. W.; Rhee, S.; Davies, D. R. The Molecular Basis of Substrate Channeling. *J. Biol. Chem.* **1999**, *274*, 12193–12196.
13. Ljungcrantz, P.; Carlsson, H.; Mansson, M. O.; Buckel, P.; Mosbach, K.; Bulow, L. Construction of an Artificial Bifunctional Enzyme, β-Galactosidase Galactose Dehydrogenase, Exhibiting Efficient Galactose Channeling. *Biochemistry* **1989**, *28*, 8786–8792.
14. Pettersson, H.; Pettersson, G. Kinetics of the Coupled Reaction Catalysed by a Fusion Protein of Beta-Galactosidase and Galactose Dehydrogenase. *Biochim. Biophys. Acta, Protein Struct. Mol. Enzymol.* **2001**, *1549*, 155–160.
15. Schoffelen, S.; Beekwilder, J.; Debets, M. F.; Bosch, D.; Hest, J. C. M. v. Construction of a Multifunctional Enzyme Complex via the Strain-Promoted Azide−Alkyne Cycloaddition. *Bioconjugate Chem.* **2013**, *24*, 987–996.
16. Lin, J.-L.; Wheeldon, I. Kinetic Enhancements in DNA−Enzyme Nanostructures Mimic the Sabatier Principle. *ACS Catal.* **2013**, *3*, 560–564.
17. Rudiuk, S.; Venancio-Marques, A.; Baigl, D. Enhancement and Modulation of Enzymatic Activity through Higher-Order Structural Changes of Giant DNA−Protein Multibranch Conjugates. *Angew. Chem., Int. Ed.* **2012**, *51*, 12694–12698.
18. Zhang, F.; Rodriguez, S.; Keasling, J. D. Metabolic Engineering of Microbial Pathways for Advanced Biofuels Production. *Curr. Opin. Biotechnol.* **2011**, *22*, 775–783.
19. Berg, H. C. *Random Walks in Biology*; Princeton University Press: Princeton, N.J., 1983.
20. Ceccarelli, E. A.; Carrillo, N.; Roveri, O. A. Efficiency Function for Comparing Catalytic Competence. *Trends Biotechnol.* **2008**, *26*, 117–118.
21. Kuhn, H.; Foersterling, H.-D. *Principles of Physical Chemistry: Understanding Molecules, Molecular Assemblies, Supramolecular Machines*; Wiley: Chichester, 1999.
22. Idan, O.; Hess, H. Diffusive Transport Phenomena in Artificial Enzyme Cascades on Scaffolds. *Nat. Nanotechnol.* **2012**, *7*, 769–770.
23. Tucker, R.; Katira, P.; Hess, H. Herding Nanotransporters: Localized Activation *via* Release and Sequestration of Control Molecules. *Nano Lett.* **2008**, *8*, 221–226.
24. Chung, Y.-H.; Xia, J.; Margulis, C. J. Diffusion and Residence Time of Hydrogen Peroxide and Water in Crowded Protein Environments. *J. Phys. Chem. B* **2007**, *111*, 13336–13344.
25. Domínguez, L.; Sosa-Peinado, A.; Hansberg, W. Catalase Evolved to Concentrate H_2O_2 at its Active Site. *Arch. Biochem. Biophys.* **2010**, *500*, 82–91.
26. Savage, D. F.; Afonso, B.; Chen, A. H.; Silver, P. A. Spatially Ordered Dynamics of the Bacterial Carbon Fixation Machinery. *Science* **2010**, *327*, 1258–1261.
27. Lizana, L.; Konkoli, Z.; Bauer, B.; Jesorka, A.; Orwar, O. Controlling Chemistry by Geometry in Nanoscale Systems. *Annu. Rev. Phys. Chem.* **2009**, *60*, 449–468.
28. Weisz, P. B. Enzymatic Reaction Sequences and Cytological Dimensions. *Nature* **1962**, *195*, 772–774.
29. Conrado, R. J.; Varner, J. D.; DeLisa, M. P. Engineering the Spatial Organization of Metabolic Enzymes: Mimicking Nature's Synergy. *Curr. Opin. Biotechnol.* **2008**, *19*, 492–499.
30. Anderson, J. B.; Carol, A. A.; Brown, V. K.; Anderson, L. E. A Quantitative Method for Assessing Co-Localization in Immunolabeled Thin Section Electron Micrographs. *J. Struct. Biol.* **2003**, *143*, 95–106.

31. An, S. G.; Kumar, R.; Sheets, E. D.; Benkovic, S. J. Reversible Compartmentalization of *De Novo* Purine Biosynthetic Complexes in Living Cells. *Science* **2008**, *320*, 103–106.
32. Beckham, G. T.; Bomble, Y. J.; Bayer, E. A.; Himmel, M. E.; Crowley, M. F. Applications of Computational Science for Understanding Enzymatic Deconstruction of Cellulose. *Curr. Opin. Biotechnol.* **2011**, *22*, 231–238.
33. Kim, D. M.; Umetsu, M.; Takai, K.; Matsuyama, T.; Ishida, N.; Takahashi, H.; Asano, R.; Kumagai, I. Enhancement of Cellulolytic Enzyme Activity by Clustering Cellulose Binding Domains on Nanoscaffolds. *Small* **2011**, *7*, 656–664.
34. Klann, M. T.; Lapin, A.; Reuss, M., Agent-Based Simulation of Reactions in the Crowded and Structured Intracellular Environment: Influence of Mobility and Location of the Reactants. *BMC Syst. Biol.* **2011**, *5*.
35. Schumb, W. C.; Satterfield, C. N.; Wentworth, R. L. *Hydrogen Peroxide*; Reinhold Pub. Corp.: New York, 1955.
36. Kamyshny, A.; Trofimova, D.; Magdassi, S.; Levashov, A. Native and Modified Glucose Oxidase in Reversed Micelles. *Colloids Surf., B* **2002**, *24*, 177–183.
37. Takegawa, K.; Fujiwara, K.; Iwahara, S.; Yamamoto, K.; Tochikura, T. Effect of Deglycosylation of N-Linked Sugar Chains on Glucose-Oxidase from Aspergillus-Niger. *Biochem. Cell Biol.* **1989**, *67*, 460–464.
38. Laberge, M.; Huang, Q.; Schweitzer-Stenner, R.; Fidy, J. The Endogenous Calcium Ions of Horseradish Peroxidase C are Required to Maintain the Functional Nonplanarity of the Heme. *Biophys. J.* **2003**, *84*, 2542–2552.
39. Violante-Mota, F.; Tellechea, E.; Moran, J. F.; Sarath, G.; Arredondo-Peter, R. Analysis of Peroxidase Cctivity of Rice (*Oryza sativa*) Recombinant Hemoglobin 1: Implications for *In Vivo* Function of Hexacoordinate Non-Symbiotic Hemoglobins in Plants. *Phytochemistry* **2010**, *71*, 21–26.
40. Kamal, J. K. A.; Behere, D. V. Activity, Stability and Conformational Flexibility of Seed Coat Soybean Peroxidase. *J. Inorg. Biochem.* **2003**, *94*, 236–242.